JOURNAL OF MATERIALS SCIENCE **33** (1998) 4697–4706

Synthesis of polymeric titanium and zirconium precursors and preparation of carbide fibres and films

H. PREISS*
TU Bergakademie Freiberg, Institut für Energieverfahrenstechnik, 09596 Freiberg, Germany
E. SCHIERHORN, K.-W. BRZEZINKA
Bundesanstalt für Materialforschung und -prüfung (BAM), 12200 Berlin, Germany

Polymeric precursors for carbothermal reactions were prepared from the chelate derivatives of titanium and zirconium alkoxides $L_2M(OR)_2$ (L is an acetylacetonato or ethyl acetoacetato group) in alcohols by reaction with organic compounds having two or more reactive OH groups, such as ethylene glycol, saccharose, tartaric acid or dihydroxybenzenes. These organic groups act as bridging ligands in transesterification and condensation polymerization yielding either spinnable viscous solutions or elastic gels. The rheological properties of the concentrated solutions allowed for the preparation of polymer fibres and films. At temperatures up to 1600 °C, bulk precursors as well as fibres and films were thermally converted into carbide powders, films or coatings. The structural transformations of the polymeric materials into the carbides were investigated using thermogravimetric–differential thermal analyses (TGA–DTA), X-ray diffraction (XRD), scanning electron microscopy (SEM), Fourier transform infra-red (FTIR) analysis and Raman spectroscopy.

1. Introduction

Polymerization of metalorganic compounds and sol–gel chemistry have proved to provide new routes to synthesize non-oxide ceramics as carbides. The precursors prepared by both techniques combine homogeneous distribution of the reactants on a colloidal or even molecular level with easy forming. Therefore, spinning and film production can be applied in principle prior to pyrolysis. The pyrolysis step then produces an amorphous residue, mostly a carbon–oxide composite, which can be easily converted into carbide. The production of transition metal carbide powders or grains has been effected from gel-derived as well as from polymeric precursors, e.g. [1, 2]. Production of these carbides in shaped forms as fibres or films, however, is reported only rarely up to now [3–5]. The shaped carbides manufactured this way contain a lot of free carbon.

Whereas sol–gel techniques have been favourable for the production of shaped oxidic ceramics, polymer routes ought to be more appropriate for non-oxidic materials. An advantage of polymeric approaches to carbide fibres or films is that they avoid certain processing problems inherent in the sol–gel routes typically used, such as: the ease of sols to transform into gels, the difficulty in controlling viscosity in sols, and the presence of a high quantity of solvents, mostly water, in the sols.

The goal of this work is to develop polymeric titanium and zirconium precursors that can be synthesized easily, shaped (e.g. by spinning, coating) by the same techniques useful for organic polymers, and transformed to the desired carbides or oxycarbides. Starting from transition metal alkoxides $M(OR)_4$, precursors are developed that are comprised preferably of linearly and not three-dimensionally connected polymers.

The tendency of transition metal alkoxides to undergo three-dimensional polymerization reactions is due to the high electrophilic character of the metal ions and to insaturation of their full co-ordination number, six–eight. Since chemical modification of the metal alkoxides by complexing is one way of reducing their reactivity to cross-linking, the alkoxides are transformed in a first step by partial derivatization to metal chelate complexes of the type $L_2M(OR)_2$, where L are bidentate ligands, e.g. β-diketones. Recently, such partial derivatization has been proved to be an effective technique for reducing the hydrolyzability of alkoxides and for synthesizing polymers with oxygen bridges that can be transformed to TiO_2 [6] and ZrO_2 [7, 8] fibres.

In the present study the approach to linear polymers is accomplished by transesterification of the OR-groups in the $L_2M(OR)_2$ derivatives with diols or other ligands having two or more reactive OH groups, and by successive condensation polymerization, whereby these additional ligands act as bridging ligands.

* *Present address: Köllnische Straße 22a, 12439 Berlin, Germany.*

The synthesis of such precursors, their spinnability and conversion to shaped carbides are described. Titanium and zirconium alkoxides are used as the starting reagents, acetylacetone (as well as ethyl acetoacetate) as chelating ligands, and diols, dihydroxybenzenes, dihydroxycarboxylic acids and saccharose as bridging ligands. The precursors and their thermal evolution are characterized by Fourier transform infra-red (FTIR) analysis and by Raman-spectroscopy, X-ray diffractometry (XRD), thermogravimetry–differential thermoanalysis (TGA–DTA) and scanning electron microscopy (SEM).

2. Experimental procedure

2.1. Preparation of the precursors

Fig. 1 presents a schematic flow chart that describes the preparation of the carbide precursors in this work. Titanium n-butoxide, $Ti(OC_4H_9)_4$ (Fluka AG), and a 70% solution of zirconium n-propoxide, $Zr(OC_3H_7)_4$, in n-propanol (Aldrich Chemie AG) were used as the starting materials. The other materials were reagent grade.

First, 0.01 mol of $Ti(OC_4H_9)_4$ or $Zr(OC_3H_7)_4$ were dissolved in 5 ml n-butanol under nitrogen in Schlenk glasswares, and the solutions were heated at 50 °C for 30 min. Then 0.022 mol of the respective diketone, acetylacetone or ethyl acetoacetate, were added dropwise at 50 °C with stirring for another 30 min; the solutions became yellow, showing that bis(diketo) alkoxides, $L_2Ti(OR)_2$ or $L_2Zr(OR)_2$, had formed. Now the hydrolyzability of the starting alkoxides is reduced and further operations can be done in open atmosphere. After the temperature of the solutions had been increased to 80 °C, materials that serve as bridging ligands were added, and the colour of the solutions changed mostly into deep red. The appropriate amounts of these bridging materials are listed in Table I (the amounts were chosen to adjust the carbon content necessary for carbide formation). Heating was continued until these materials had dissolved. In some cases, especially when saccharose was used as the bridging ligand, this took about 1–2 h. Afterwards the solutions were heated up to the reaction temperatures given in Table I and concentrated at these temperatures; sometimes the solutions had already become spinnable through concentration. Evaporation of the solvents, mainly butanol, led to neat precursors, which were used for testing their spinnability (the ability to form fibres of films), pyrolysis behaviour and structural characterization. Occurrence of spinnability was estimated by hand-drawing fibres from precursor solutions.

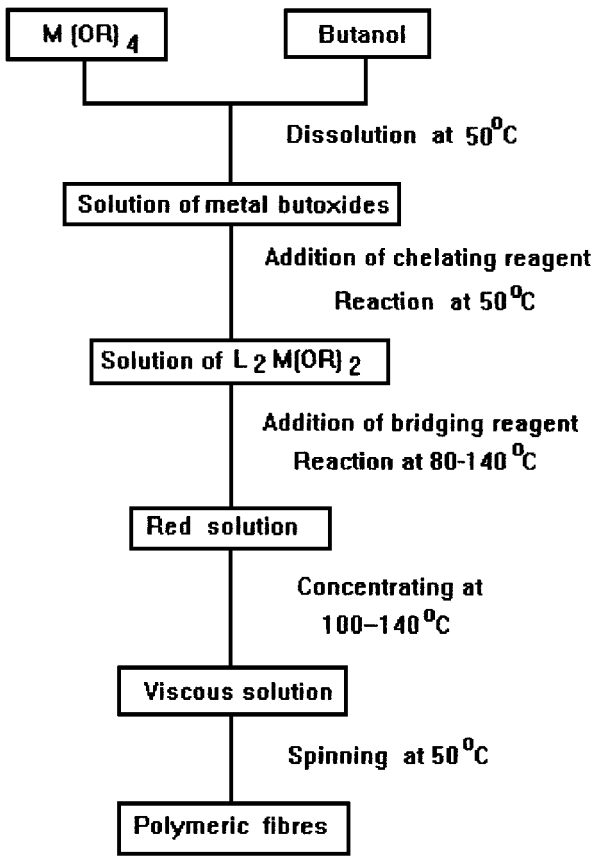

Figure 1 Scheme of the experimental procedure used for the fabrication of polymeric precursor fibres.

2.2. Heat treatment

The bulk precursors as well as the fibres and coated substrates were annealed in alumina boats using an alumina tube furnace (Carbolite Furnace Limited) at 300–1550 °C with 50 or 100 °C intervals in flowing argon. The heating rate was adjusted to 5 °C min^{-1}, and the holding time at the maximum temperature was 1 h.

2.3. Characterization methods

The thermal behaviour of the bulk precursors in argon atmosphere was studied up to 1600 °C by simultaneous TGA–DTA using a Setaram TAG 24 thermoanalyser. The heating rate was 10 °C min^{-1}.

Conventional FTIR and XRD (CuK_α) were used to record the infra-red (i.r.) spectra and X-ray diffractograms.

Raman scattering experiments were carried out with a Dilor XY laser Raman spectrometer in back scattering geometry using the micro-Raman technique (Olympus microscope model BH2 50x) with a nitrogen cooled CCD camera multichannel detector. All spectra were recorded at room temperature and atmospheric conditions with the 514.5 nm line of an argon ion laser (CZ-model ILA 120) for excitation. The laser power was < 10 mW with a power intensity of approximately < 100 kW cm^{-2} on the sample surface. The integration time was 1–1000 s and the resolution 1 cm^{-1}.

Carbon analyses of the heat-treated bulk precursors were performed using the CHN-analyser EA 1110 (CE Instruments). The microstructure of the surface and the cross-section of the heat treated fibres were observed by SEM.

3. Results and discussion

3.1. Preparation of the precursors

The basic reactions occurring during precursor formation are metal chelate formation, transesterification and condensation polymerization. During reaction of

TABLE I Properties of polymer precursors with various chelating and bridging ligands

Polymer type[a,b]	Quantity of bridging ligand/0.01 mol $M(OR)_4$ (g)	Reaction temperature (°C)	State of concentrated polymer solution	Spinning solvent[c]	Carbon content at 800 °C (wt %)
TiAGl	0.30	120	Spinnable	Bu, Pr	28.8
TiEGl	0.30	80	Elastic gel		25.5
TiASa	0.60	140	Spinnable	Bu, Pr, Be, To	32.8
TiESa	0.70	145	Spinnable	Bu, Pr, Be,	31.3
TiATt	1.50	120	Spinnable	Bu, Pr, Et, Be, To	30.3
TiETt	1.50	140	Spinnable	Pr	29.8
TiACa	0.48	120	Spinnable	Pr, To	32.7
TiAHy	0.40	125	Spinnable	Bu, Pr	31.6
TiARe	0.35	125	Spinnable	Pr, To	36.1
TiECa	0.60	130	Spinnable	Bu, Be, To	32.3
TiEHy	0.50	60	Elastic gel		34.0
TiERe	0.50	135	Spinnable	Be, To	30.8
ZrAGl	0.70	r.t.	Spontaneous gel		17.8
ZrEGl	0.70	r.t.	Spontaneous gel		19.1
ZrASa	0.65	130	Spinnable gel	Et	22.6
ZrESa	0.80	130	Spinnable gel	Be	22.3
ZrATt	1.50	80	Precipitate		
ZrETt	1.50	80	Precipitate		
ZrACa	0.48	110	Spinnable	Bu, Pr	23.5
ZrAHy	0.36	110	Spinnable	Pr, Et	24.9
ZrARe	0.36	110	Spinnable	Pr, Et	26.6
ZrECa	0.50	110	Spinnable	Pr	24.3
ZrEHy	0.36	110	Spinnable	Bu, Pr, Et	22.6
ZrERe	0.36	110	Spinnable	Pr, Et	22.0

[a]Chelating ligand: A, acetylacetone; E, ethyl acetoacetate.
[b]Bridging ligand: Gl, ethylene glycol; Sa, saccharose; Tt, tartaric acid; Ca, catechol; Hy, hydroquinol; Re, resorcinol.
[c]Bu, n-butanol; Pr, n-propanol; Et, ethanol; Be, benzene; To, toluene.

the alkoxides with the diketones, co-ordination expansion of the metal atoms up to six occurs and the bis(diketo) alkoxides $L_2M(OR)_2$ (L is an acetylacetato or ethyl acetylacetato group) are formed. Here, the diketones clearly behave as chelating ligands. Since the full co-ordination number, i.e. six-eight, of these metals is usually not satisfied in monomeric transition metal alkoxides $M(OR)_4$, they are mostly (e.g. in non-polar solvents) associated via alkoxy bridges to polymeric units. The titanium and zirconium alkoxides with primary alkoxy groups form trimeric species with pentaco-ordinated metal atoms [9]. In polar solvents, such as alcohols, co-ordination expansion occurs by solvatation. Complexing by chelating ligands, however, satisfies the full co-ordination number and reduces reactivity of the derivatives, also against hydrolysis. Consequently, the ligands originally incorporated lend moisture stability to the precursors.

The formation of polymeric precursors can be accomplished by succeeding condensation reactions with compounds that have two or more reactive OH groups, such as diols, dihydroxybenzenes, polysaccharides and dihydroxycarboxylic acids, and behave as bridging ligands. We assume that carboxylic acids may behave as chelating ligands, too. Recently, it has been reported that carboxylic acids act with alkoxides both as bridging and chelating ligands [10]. The condensation can mostly be divided in two steps: the transesterification of alkoxy groups in $L_2M(OR)_2$ derivatives according to Equation 1

$$n\text{-RO}-\underset{\text{acac}}{\overset{\text{acac}}{\text{Ti}}}-\text{OR} + n\text{-HO}-\text{X}-\text{OH} \rightarrow n\text{-RO}-\underset{\text{acac}}{\overset{\text{acac}}{\text{Ti}}}-\text{O}-\text{X}-\text{OH} + n\text{-ROH} \quad (1)$$

where acac is acetylacetone and X is the bridging ligand; and second, polycondensation of the intermediates according to Equation 2

$$n\text{-RO}-\underset{\text{acac}}{\overset{\text{acac}}{\text{Ti}}}-\text{O}-\text{X}-\text{OH} \rightarrow -\left[-\text{O}-\underset{\text{acac}}{\overset{\text{acac}}{\text{Ti}}}-\text{O}-\text{X}-\right]_n- + n\text{-ROH} \quad (2)$$

Transesterification in the solution is often accompanied by a change of colour. The colour of the solution of $(acac)_2\ Ti(OC_4H_9)_2$ in butanol, for instance, changes to deep red when saccharose or resorcinol is added at

80 °C. An orange colour is obtained for the zirconium analoga. Formation of the polymers needs higher reaction temperatures (Table I) than transesterification, although both reactions are mostly interlocked. There is an increase in solution viscosity as a function of temperature and time, which we ascribe to polycondensation.

Parallel to transesterification–condensation, self-condensation reactions of the type described by

$$m\text{-RO}-\underset{\text{acac}}{\overset{\text{acac}}{\text{Ti}}}-\text{OR}\rightarrow-\left[\begin{array}{c}\text{acac}\\ -\text{Ti}-\text{O}-\\ \text{acac}\end{array}\right]_m-+\ m\text{-ROR} \quad (3)$$

may also occur. Self-condensation reactions, according to Equation 3, give rise to polymeric metaloxan structures. Under heating at maximum reaction temperatures, solvents as well as alcohol and ether, produced according to Equations 1–3, are evaporated leading first to concentrated and sometimes spinnable solutions and finally to neat precursors. Presumably, the concentrated solutions contain cyclic as well as linearly connected polymers. If the viscous solutions are spinnable, however, it seems reasonable to consider that the precursors exist mostly as linear structures, which can have both Ti–O–Ti and Ti–O–X–O–Ti bridges.

In some cases, especially for dihydroxybenzenes as bridging ligands, condensation reactions are incomplete because they are slow at the reaction temperatures. Thus, polymerization reactions, which require full elimination of OH and OR groups, will occur at higher temperatures (150–350 °C). The systems are complicated, as precursor degradation will occur simultaneously (see Section 3.3).

Equations 1–3 are idealized in giving rise to linearly connected polymers and the occurrence of spinnability. It should be borne in mind that during concentration of the solutions, the polymers may also aggregate to a more or less three-dimensionally connected network polymer, which gives the solution either an elastic nature or cause spontaneous transformation into a gel. Such gelling phenomena can be due to the low complexing ability of chelating ligands and/or to high reactivity of the alkoxides with the bridging ligands. Then, the bridging ligands partially substitute for the diketone ligands and give rise to three-dimensional condensation. In order to avoid this condensation we used a diketone: alkoxide molar ratio of 2.2 instead of 2.0. Nevertheless, the results in Table I show that gelling could not be ruled out in all cases. The alkoxide derivatives react particularly with ethylene glycol to form gel products.

3.2. Spinnability and film production

Prior to examination of their spinnability the precursors were tested for solubility in common solvents. It has been proved that most of the precursors are soluble both in polar solvents (alcohols), and non-polar solvents, such as benzene and toluene (see Table I). The precursors that resulted as precipitates or spontaneous gels are no more soluble. Upon concentrating the solutions, they turned either into elastic gels or viscous solutions, which exhibit rheological properties that allow the formation of fibres. The concentration dependence of the viscosity supports the assumption that the precursors exist preferentially as linear polymers.

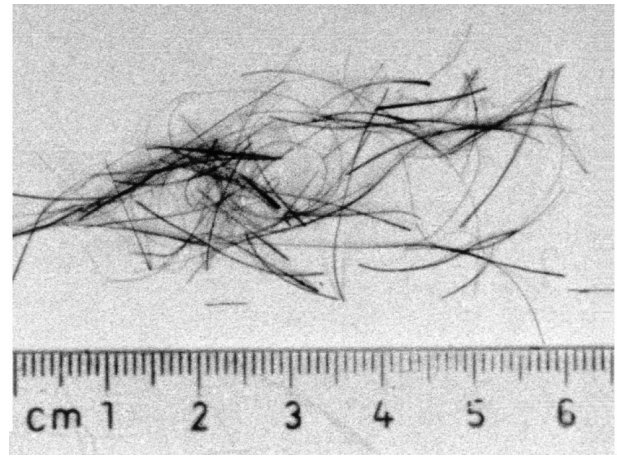

Figure 2 Macroscopic appearance of TiERe polymer fibres as-synthesized.

Fibres were hand-drawn by extracting a glass rod from the viscous solutions at 40–50 °C. Sometimes solutions of an elastic nature also showed the occurrence of spinnability before they gelled, e.g. precursor TiEHy was only spinnable immediately after its synthesis. Spinnability was estimated by the length of the drawn fibres (spinnability in Table I means that fibres of a length of >20 cm could be drawn). Since the fibres are more or less thermoplastic and may deform upon drying, they were suspended on a glass bar and dried at room temperature for one week before they were pyrolysed.

Fig. 2 gives an example of the appearance of the TiERe polymer fibre after drying. However, in some cases, e.g. for TiACa, TiAHy and TiARe, the plasticity of the fibres was so high that the fibres did not maintain their original shape.

The occurrence of spinnability can also be applied to the fabrication of polymer films and carbide coatings. For film preparation, precursor solutions of a lower viscosity than for fibre drawing were used. Alumina foams were immersed in approximately 20 wt % precursor solution of TiASa in butanol or ZrAHy in benzene, and slowly extracted. After drying, first at room temperature for one day and then at 150 °C for 1 h, the films were pyrolysed under argon up to 1550 °C.

3.3. Thermal decomposition of the precursors

TGA, differential thermogravimetric analysis (DTG) and DTA curves of the precursors TiERe and ZrERe are given in Figs 3 and 4. The thermal results of these samples are typical for all the precursors studied. All TGA curves can be roughly divided into three sections: a first dramatic mass loss caused by decomposition of the precursor, a following section of nearly constant mass, and finally a mass loss corresponding to carbothermal reduction.

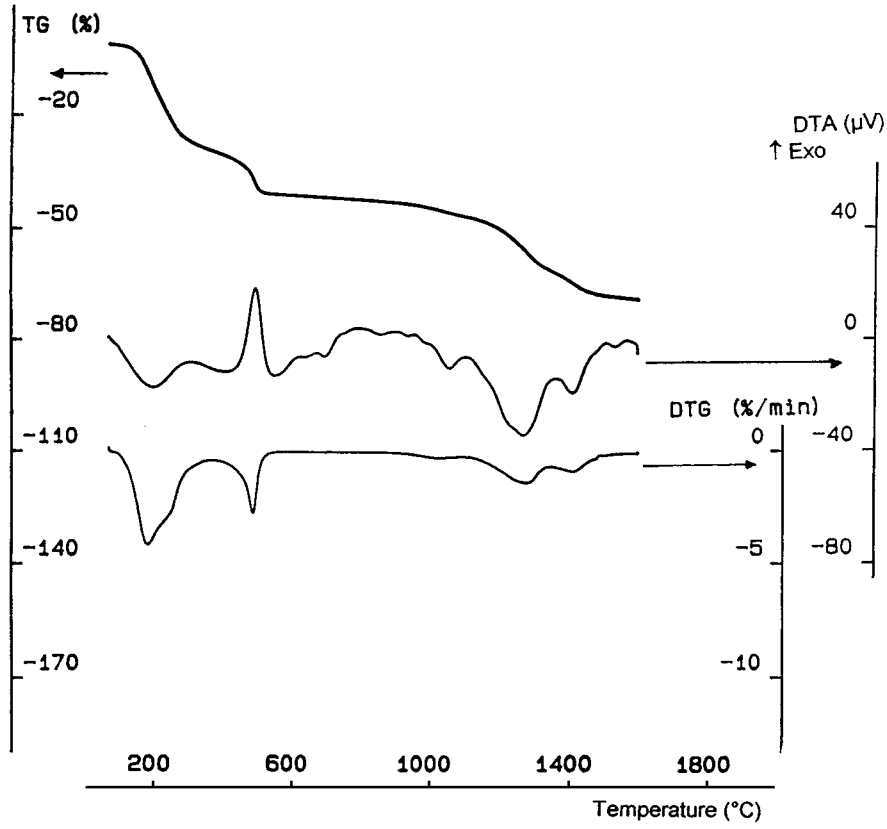

Figure 3 TGA, DTGA and DTA curves of TiERe precursor obtained under argon.

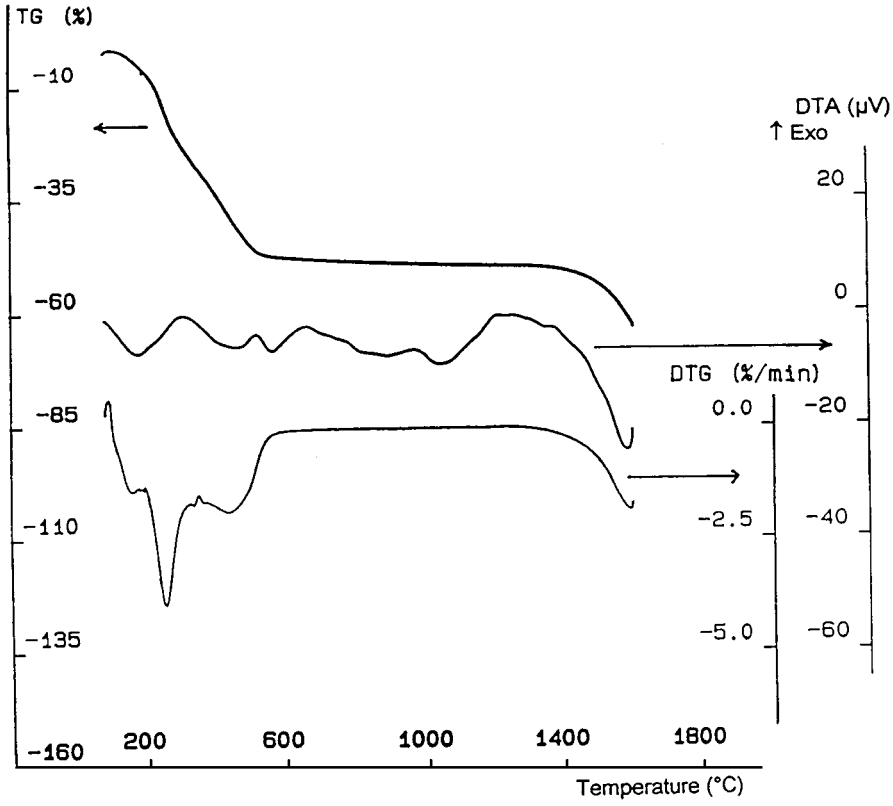

Figure 4 TGA, DTGA and DTA curves of ZrERe precursor obtained under argon.

The decomposition reactions start with the loss of residual solvents and organic byproducts at approximately 100 °C and end at approximately 550 °C. The first DTGA-mass-loss peaks at 200–300 °C for both samples are likely due to the release of alcohol and ether during completion of the condensation polymerization. FTIR investigations support this assumption.

Figs 5 and 6 show the i.r. spectra for the as-synthesized TiERe and ZrERe precursors, and for both precursors after annealing at 350 °C for 1 h. Both

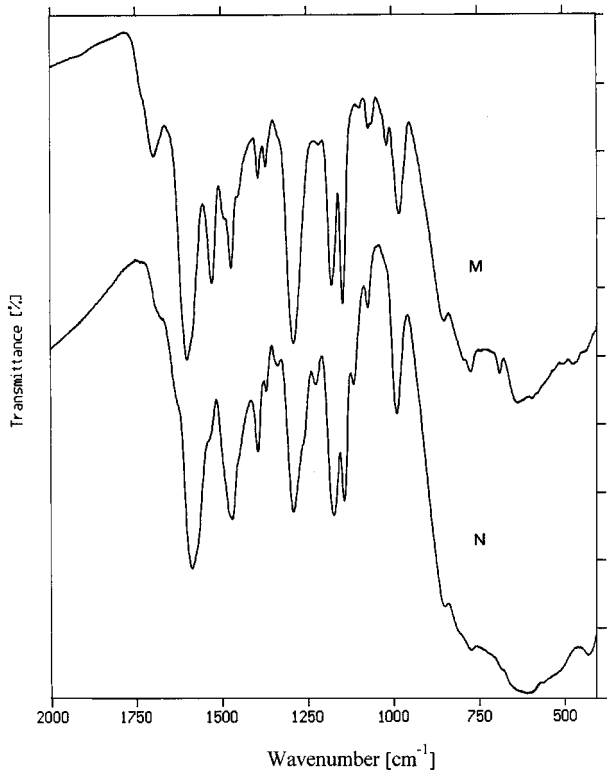

Figure 5 FTIR spectra of TiERe precursor after drying at 125 °C (M) and heating at 350 °C (N).

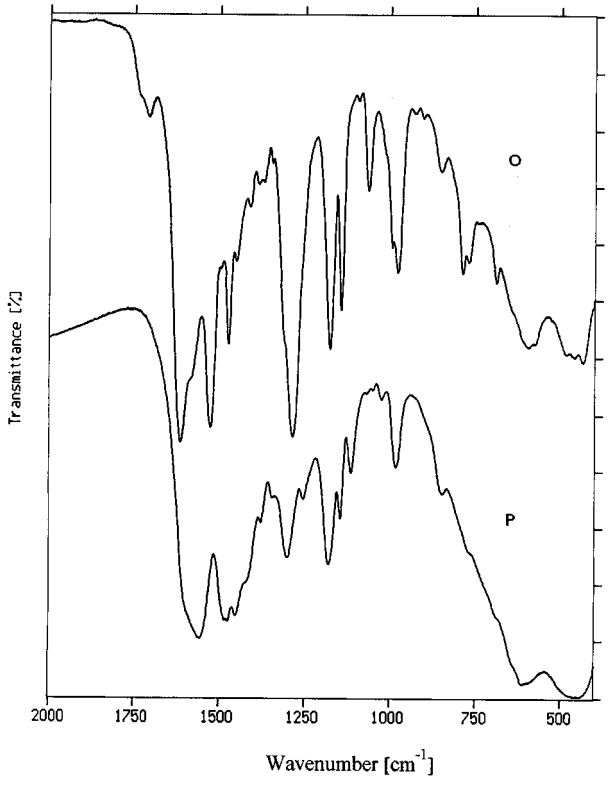

Figure 6 FTIR spectra of ZrERe precursor after drying at 110 °C (O) and heating at 350 °C (P).

starting compounds exhibit strong absorption bands at 1500–1600 cm^{-1}, corresponding to C=C and C=O vibrations, and a series of bands at 1200–1400 cm^{-1}, corresponding to C–C and (CH) bending vibrations. These bands are ascribed to the chelating and bridging ligands. Weak bands between 1000 and 1100 cm^{-1} may be assigned to vibrations of C–O bonds, where O is attached to the metal atoms in alkoxides [11, 12]. The broad i.r. signal at the low energy side of the spectra (<900 cm^{-1}) should be due to an envelope of bands of different Ti–O–Ti or Zr–O–Zr bonds. The i.r. spectra of the products after annealing at 350 °C are similar to those of the starting materials; we still see most of the previous bands. It is more interesting, however, to notice that the bands at 1016 and 1060 cm^{-1}, typical of C–O vibrations in the titanium alkoxide, and 1000 and 1065 cm^{-1}, typical of C–O in the zirconium alkoxide, have disappeared. Moreover, the broad bands below 900 cm^{-1} become more intensive and broader, indicating the more polymeric nature of the annealed products.

The DTA curves in Figs 3 and 4 reveal endothermic signals in the range 100–350 °C, as expected for pyrolysis of organic material. At approximately 500 °C, an exothermic peak is observed for the precursors. Since this peak corresponds with the termination of the decomposition reaction, it is assumed that this exothermal effect is associated with the formation of an amorphous carbon–oxide composite.

In the temperature ranges 550–950 °C for titanium and 550–1100 °C, for zirconium precursors, a mass loss of approximately 2% and no thermal effects indicative of crystallization are observed. XRD, however, exhibits the beginning of TiO_2 crystallization (anatase) and of a ZrO_2 metastable cubic form at 700 °C. It has to be noted that similar crystallization processes, leading to these oxide phases with particles of nanometre size, have been found for gel-derived zirconium and titanium precursors at the same temperature [1, 13].

The results of carbon analyses of the carbon–oxide composites obtained after pyrolysis at 800 °C are listed in Table I. They are close to the theoretical values needed for carbothermal formation of TiC (31.06 wt %) and ZrC (22.61 wt %).

3.4. Crystallization and Raman spectroscopy

Raman spectroscopy was used as an complementary method to XRD because it has been proven to be an effective technique for following the thermal evolution of amorphous TiO_2 materials [14–20]. In general, Raman spectroscopy is more sensitive to shorter-range order than XRD. In this work, Raman spectroscopy was applied to record spectra of thermally treated samples as well as to accomplish crystallization photochemically and thermally caused by the laser beam. In the latter case, laser power was increased either by increasing laser energy or by stepwise focusing of the laser beam.

Fig. 7 shows Raman spectra recorded for the as-synthesized TiERe precursor dried at 125 °C, and Fig. 8 shows spectra of this precursor after heat treatment at 700 °C. The spectrum of the as-synthesized material (Fig. 7a) shows bands at 291 (very weak), 506 (very weak), 594 and 666 cm^{-1}, which we ascribe to precursor bands. In the spectrum of the precursor annealed at 350 °C (not depicted in this work) these bands are still present, showing incomplete decomposition at this

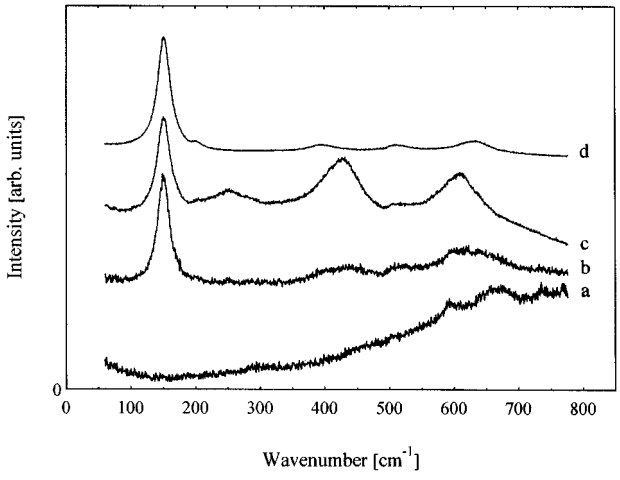

Figure 7 Raman spectra of the as-synthesized TiERe precursor measured with increased focusing of the laser beam from (a) to (d).

temperature. With increased power of the laser by focusing, the precursor bands disappear and some new bands, an intensive one at approximately 150 cm^{-1} and two broad bands at approximately 420 and 620 cm^{-1}, are observable (Fig. 7b). The frequency of the most intensive band lies close to that of the E_g mode of anatase. The other two bands, lying closer to the A_{1g} and E_g mode of crystalline rutile (612 and 448 cm^{-1}, see [15]), have been recently found for amorphous TiO_2 [14–17] and for nano crystalline TiO_2 [18, 19]. These bands have been suggested as being derived from short-range ordered TiO_6 units without the long-range order of crystalline anatase or rutile.

All the new bands intensify when the laser beam is more sharply focused (Fig. 7c). Fig. 7c also shows a band at approximately 250 cm^{-1}, which is always observed for rutile; its assignment, however, is not yet clear [18, 20]. Finally, the Raman spectrum of the amorphous or nano phase TiO_2 changes into that of anatase by further focusing (Fig. 7d). Recently, such spectral transformation has also been observed with thermal heating processes [15–17].

After pyrolysing the titanium precursor at 700 °C for 1 h, the Raman spectrum in Fig. 8a shows no more characteristic features for the precursor < 800 cm^{-1} peak.

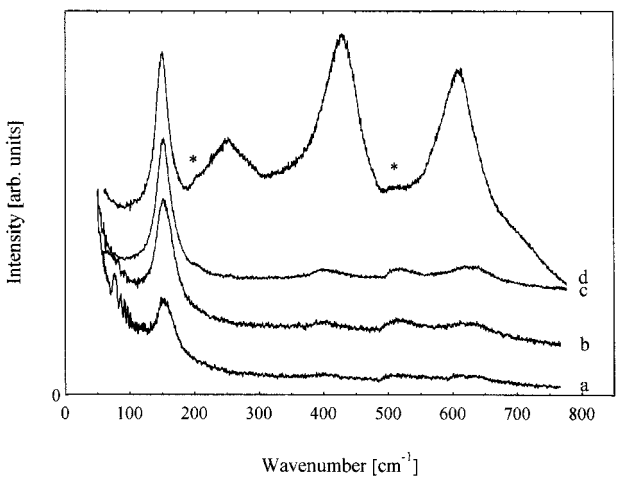

Figure 8 Raman spectra of the 700 °C annealed TiERe precursor measured with increased focusing of the laser beam from (a) to (d).

Some weak bands at 150, 430 and 640 cm^{-1}, which may be attributable to anatase and/or nanophase TiO_2, and two intensive lines at 1350 and 1590 cm^{-1}, which can be assigned to the G and D line of pre-graphitized carbon, are observable. These findings correspond with XRD results, revealing, at 700 °C, broad diffraction lines indicative of nanocrystalline TiO_2 in anatase form. By successive focusing of the laser beam, the spectrum changes, as shown sequential from Fig. 8a–d, demonstrating the crystallization progress of anatase and its phase transformation. The observable frequencies in Fig. 8c correspond with those of anatase single crystals (147, 198, 398, 515, 640 cm^{-1}, see [15]) and the final spectrum in Fig. 8d reveals the presence of rutile, only traces of anatase could still be detected (weak anatase lines are marked by an asterisk).

The Raman spectrum of the ZrERe precursor, recorded immediately after focusing the laser beam, did not reveal Raman features either for the as-synthesized nor the 350 °C annealed sample. These findings are surprising because characteristic i.r. spectra could be obtained from these samples (see Fig. 6). An explanation may be that FTIR spectroscopy is more sensitive to short-range order. The Raman spectrum of the precursor annealed at 700 °C for 1 h is characterized by a low "background" and a broad band centred at approximately 620 cm^{-1} (Fig. 9a). Presumably, this band is assignable to cubic ZrO_2 [21, 22], which was crystallized according to the XRD results as nanometre-sized particles within the carbon matrix. Recently, it has been found that gel-derived precursors also reveal broad XRD peaks at 2θ ranges where cubic and tetragonal ZrO_2 have the most intensive peaks [1]. Moreover, it has been stated that this metastable ZrO_2 in the carbon–zirconia composite transforms at further heating into tetragonal (t) and monoclinic (m) ZrO_2. Here, the polymer precursors show similar crystallization phenomena by increasing the laser energy. The polymer precursor annealed at 350 °C for 1 h needs an energy increase from 10 to 25 mW to accomplish phase transformation into a mixture of t- and m-ZrO_2 (Fig. 9b). The precursor previously annealed at 700 °C needs an energy increase

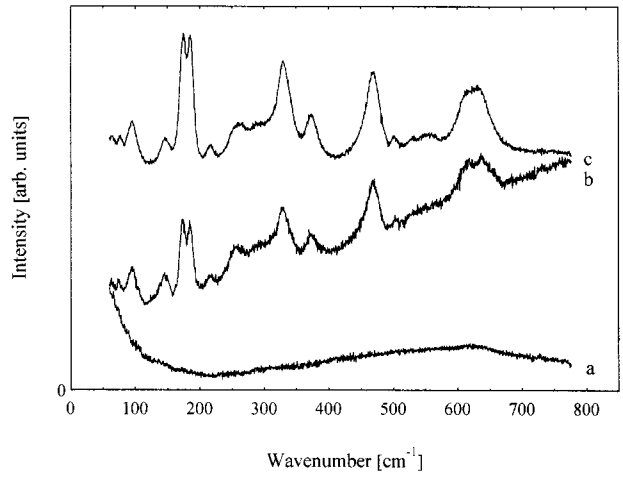

Figure 9 Raman spectra of the ZrERe precursor: annealed at 700 °C and measured with a laser energy of 10 mW (a); annealed at 350 °C and measured with a laser energy of 25 mW (b); annealed at 700 °C and measured with a laser energy of 50 mW (c).

upto 50 mW for this transformation (Fig. 9c). Fig. 9b, c shows that t-ZrO_2 (Raman lines 146, 256, 312, 461 and 646 cm^{-1}) and m-ZrO_2 (Raman lines 175, 186, 327/343, 376 and 471 cm^{-1}) are present side by side.

The Raman results clearly demonstrate that crystallization processes for titanium precursors take place in the sequence amorphous TiO_2 → nano phase TiO_2 → anatase → rutile and for the zirconium precursors in the sequence amorphous ZrO_2 → nanophase c-ZrO_2 → metastable t-ZrO_2 → m-ZrO_2.

3.5. Carbothermal reduction of bulk precursors

Upon heat treatment, carbon–oxide composites undergo phase transformations, already found by Raman spectroscopy, before the onset of carbothermal reduction. Anatase transforms at 800–900 °C into rutile, and metastable c/t-ZrO_2 into m-ZrO_2 at 1000–1100 °C. Reduction begins for the different titanium precursors at nearly the same temperature approximately (950 °C), and for the zirconium precursors at approximately 1300 °C, as demonstrated by the TGA curves in Figs 3 and 4.

More details of the reduction reactions in titanium precursors are visible on the DTGA curve in Fig. 3, which shows that carbothermal reduction proceeds in three steps between 950 and 1600 °C. This three-step mechanism has also been found for reduction reactions in gel-derived precursors [13], and could be assigned according to XRD results, to

1. The reduction of rutile to Ti_4O_7 and Ti_3O_5.
2. The formation of titanium oxycarbide.
3. Substitution of O by C in the oxycarbide.

By using XRD the same reaction sequence was proved for the polymer precursors (the XRD patterns are not depicted in this paper).

For the zirconium polymer precursors no multistep reduction mechanism was detected neither with the DTA nor the DTG curves. This behaviour corresponds with the fact that no zirconium suboxides are known. XRD exhibits, for the final heating products, diffraction lines of B1 rock-salt type, which we ascribe to zirconium oxycarbide.

Although chemical analyses of the 800 °C pyrolysis products satisfy the carbon amounts required for the formation of stoichiometric TiC and ZrC we have to assume that the final heating products are composed simultaneously of oxycarbides and free carbon. Preparing pure TiC and ZrC is very difficult and requires much higher temperatures than used here. The carbon contents for the titanium polymer precursors heated at 1550 °C are between 25 and 28 wt % (theoretical for TiC: 20.03 wt %), and for the zirconium precursors between 13 and 16 wt % (theoretical for ZrC: 11.63 wt %).

3.6. Carbothermal reduction of polymer fibres and films

Fibre stability is the most important criterion for the conversion of polymeric fibres into carbide fibres, and it is mostly effected by shrinkage processes and the expulsion of organic materials. The TGA curves in Figs 3 and 4 show two critical temperature ranges: the range of the pyrolysis reactions leading to oxide–carbon composites, and that of the carbothermal reductions, reaching from about 950 upto 1600 °C. It has been found that the pyrolysis reactions accompanied by a mass loss of approximately 40% more detrimentally affect the fibre stability than the carburization reactions. Fibres obtained after pyrolysis suffer from shrinkage damage and fragility, however, no further deformation have been observed during the carbothermal reactions. The macroscopic appearance of zirconium carbide fibres obtained from a ZrECa precursor at 1550 °C is shown in Fig. 10.

Fig. 11 shows an alumina foam with and without a titanium oxycarbide coating prepared from a TiASa precursor. The coating procedures rendered the ceramic foams electrically conductive. Ohmic resistances of 4–5 Ω were measured between two points with a distance of 3.5 cm, showing nearly metallic conductivity of the foams.

The quality of the carburized fibres was additionally investigated using SEM. The SEM micrograph of

Figure 10 Macroscopic appearance of carbide fibres obtained from ZrECa precursor after annealing at 1550 °C.

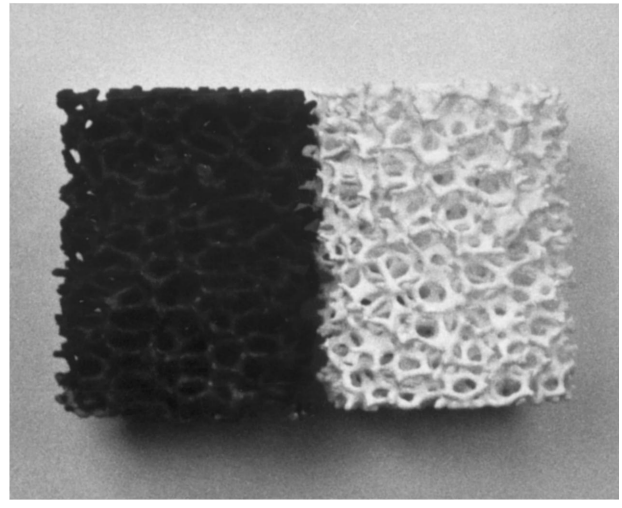

Figure 11 Ceramic foam before and after coating with titanium oxycarbide.

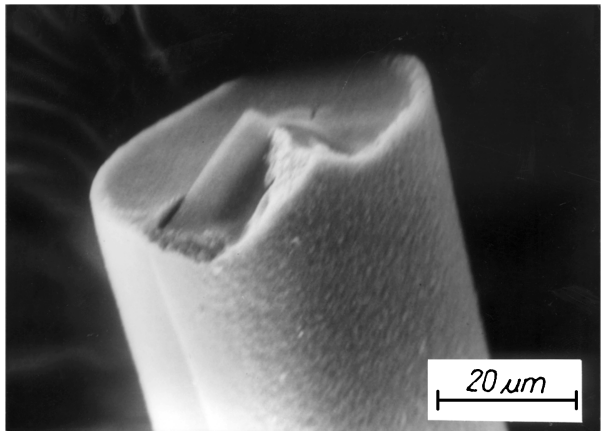

(a)

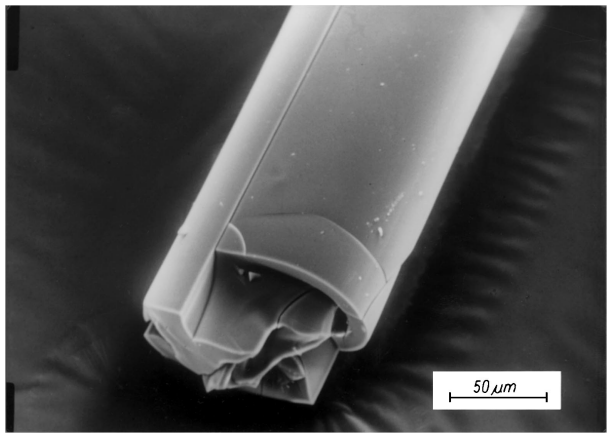

(b)

Figure 12 Electron micrographs of surfaces and cross-sections of fibres obtained from ZrECa (a), and TiATt (b) at 1550 °C.

a fibre obtained from ZrECa after annealing at 1550 °C (Fig. 12a) shows that in general dense fibres with a circular cross-section and diameters of approximately 50 μm could be produced. They consist of sintered submicrometre-sized grains. The fibres of the heated titanium precursors mostly exhibit a smooth surface. In some cases, even microcracks originate from shrinkage processes and reaction products evolve. Fig. 12b shows a typical crack running along the axis of a carbide fibre produced from a TiATt precursor. In order to clarify the optimum conditions of the drying, pyrolysing and carbidizing processes, further studies are needed because only a limited number of experiments were examined in the present work.

4. Conclusions

Gelling readily occurs when titanium or zirconium alkoxides react with water, ethylene glycol, glycerol or saccharose in alcoholic solutions. Stable solutions, however, are obtained in the presence of acetylacetone or ethyl acetoacetate. This is due to the complexing ability of the diketo ligands, which partially substitute OR groups and behave as chelating ligands. In such derivatives six-fold co-ordination of the metals is satisfied, allowing a slow-down of the system's reactivity. Therefore, chemical modification of titanium and zirconium alkoxide to derivatives of the type $L_2M(OR)_2$ is one way for the formation of preceramics by solution routes. The controlled exchange of OR groups by organic compounds, which have two or more reactive OH groups and behave as bridging ligands (ethylene glycol, saccharose, tartaric acid, dihydroxybenzenes), was investigated, and it has been found that either viscous solutions or elastic gels could be obtained. It is to be assumed that three-dimensional gel networks are formed when either the bridging ligands (e.g. ethylene glycol) have a high nucleophilic nature and substitute for the chelating ligands, or when the full co-ordination number is not satisfied in the solution.

In most cases studied here, condensation polymerization by bridging ligands has been successfully employed in the preparation of spinnable precursors. The viscosity of their solutions exhibit concentration dependence, which may be characterized by the presence of linear polymers. This is interpreted to be the reason for the occurrence of spinnability. Polymer films and hand-drawn fibres can be prepared and thermally converted into carbide coatings and fibres. Thermoplasticity, evolution of organic byproducts during pyrolysis, and pore generation during the carbothermal reduction are detrimental, causing fibre deformation and brittleness. Modifying the drying and pyrolysis processes by slow heating was successful in some cases only. In order to clarify the optimum synthesis and heating conditions for fibre production further studies are needed.

Carbide coatings are more easily obtainable from the precursor solutions. Alumina foams coated with polymer films and heat treated at 1550 °C exhibit an electrical conductivity close to that of metals. It is thought that such materials are applicable as ceramic filters, catalysts or catalyst supports.

Acknowledgements

The authors wish to thank Dr Reklat (BAM) for FTIR and Dr Schultze (BAM) for TGA–DTA experimental work.

References

1. H. PREISS, L.-M. BERGER and K. SZULZEWSKY, *Carbon* **34** (1996) 109.
2. Z. JIANG and W. E. RHINE, *Chem. Mater.* **3** (1991) 1132.
3. Y. KUROKAWA, H. OTA and T. SATO, *J. Mater. Sci. Lett.* **13** (1994) 516.
4. K. THORNE, S. J. TING, C. J. CHU, J. D. MACKENZIE, T. D. GETMAN and M. F. HAWTHORNE, *J. Mater. Sci.* **27** (1992) 4406.
5. M. NARISAWA, S. KIDA, T. DIMOO, K. OKAMURA and Y. KURACHI, *J. Sol–Gel Sci. Technol.* **4** (1995) 31.
6. W. C. LACOURSE and S. KIM, in "Science of Ceramic Chemical Processing", edited by L. L. Hench and D. R. Ulrich (Wiley, New York, 1986) p. 304.
7. T. YOGO, *J. Mater. Sci.* **25** (1990) 2394.
8. H. GOTO, H. TOMIAKA, T. GUNJI, Y. NAGAO, T. MISONO and Y. ABE, *J. Ceram. Soc. Jpn* **101** (1993) 336.
9. F. BABONNEAU, S. DOEUFF, A. LEAUSTIC, C. SANCHEZ, C. CARTIER and M. VERDAGUER, *Inorg. Chem.* **27** (1988) 3166.
10. S. DOEUFF, M. HENRY, C. SANCHEZ and J. LIVAGE, *J. Non-Cryst. Solids* **89** (1987) 206.
11. H. KRIEGSMANN and K. LICHT, *Z. Elektrochem.* **62** (1958) 1163.

12. R. W. ADAMS, R. L. MARTIN and G. WINTER, *Aust. J. Chem.* **20** (1967) 773.
13. H. PREISS, L.-M. BERGER and D. SCHULTZE, *J. Eur. Ceram. Soc.* submitted.
14. G. J. EXARHOS, *MRS Symp. Proc.* **48** (1985) 461.
15. M. OCANA, J. V. GARCIA-RAMOS and C. J. SERNA, *J. Amer. Ceram. Soc.* **75** (1992) 2010.
16. P. K. DUTTA, P. K. GALLAGHER and J. TWU, *Chem. Mater.* **4** (1992) 847.
17. K. TERABE, K. KATO, H. MIYAZAKI, S. YAMAGUCHI, A. IMAI and Y. IGUCHI, *J. Mater. Sci.* **29** (1994) 1617.
18. C. A. MELENDRES, A. NARAYANASAMY, V. A. MARONI and R. W. SIEGEL, *J. Mater. Res.* **4** (1989) 1246.
19. J. C. PARKER and R. W. SIEGEL, *ibid.* **5** (1990) 1246.
20. WU XIJUN, ZHANG MING-SHENG, YIN ZHEN, JI XIAOLI and CHEN QIANG, *Chin. Phys. Lett.* **11** (1994) 685.
21. S. SHIN and M. ISHIGAME, *Phys. Rev. B* **34** (1986) 8875.
22. M. ISHIGAME and E. YOSHIDA, *Solid State Ionics* **23** (1987) 211.

Received 17 April
and accepted 18 June 1998